

## Non-linear MHD modelling of Edge Localized Modes dynamics.

<sup>1</sup>M.Bécoulet, <sup>2</sup>M. Kim, <sup>3</sup>G. Yun, <sup>4</sup>S. Pamela, <sup>1,5</sup>G.T.A.Huijsmans, <sup>6</sup>J.Morales, <sup>1</sup>X.Garbet,  
<sup>1</sup>C.Passeron, <sup>1</sup>O.Février, <sup>7</sup>M.Hoelzl, <sup>7</sup>A.Lessig, <sup>7</sup>F. Orain

<sup>1</sup>CEA, IRFM, 13108 Saint-Paul-Lez-Durance, France

<sup>2</sup>Ulsan National Institute of Science and Technology (UNIST), 44919, Ulsan, Rep. of Korea

<sup>3</sup>Pohang University of Science and Technology, Pohang, Gyeongbuk 790-784, Rep. of Korea

<sup>4</sup>CCFE, Culham Science Centre, Oxon, OX14 3DB, UK Abingdon, UK

<sup>5</sup>Eindhoven University of Technology, Eindhoven, The Netherlands

<sup>6</sup>EPFL SB CRPP CRPP-TH, CH-1015, Lausanne, Suisse

<sup>7</sup>Max Planck Institute for Plasma Physics, Boltzmannstr. 2, 85748 Garching, Germany

[marina.becoulet@cea.fr](mailto:marina.becoulet@cea.fr)

**Abstract.** The dynamics of ELMs observed using Electron Cyclotron Emission Imaging (ECEI) on KSTAR tokamak is compared to the modelling results using the non-linear reduced resistive MHD code JOEAK for KSTAR pulse parameters and geometry including X-point and Scrape Off Layer (SOL). The full ELM crash modelling was performed for single and multi-harmonic representation and in multi-cycles ELMy regimes. The most unstable toroidal modes numbers ( $n=5-8$ ), velocity ( $\sim 5\text{km/s}$  for  $n=8$  mode) and the direction of the mode rotation were reproduced in the JOEAK modelling. The two fluid diamagnetic effects and toroidal rotations included in the JOEAK model were found to be the most important factors in explaining the experimentally observed rotation of the ballooning modes before the ELM crash and in the inter-ELM phase. In multi-harmonic multi-cycle simulations the spectrum of temperature fluctuations is similar to the experimental one in the inter-ELM phase, where several rotating modes with medium  $n$  numbers were detected in 5-30kHz frequency range. These coherent rotating structures seen in modelling are similar to the experimentally observed and can contain single or several harmonics which last from 0.2ms to few ms in time, can appear and disappear in the inter ELM period or persist until a new ELM crash.

**1.Introduction.** The understanding of Edge Localized Modes (ELMs) physics is of great importance for ITER where heat and particles fluxes due to ELMs represent concern for plasma facing components (PFC) [1]. With this respect the development and direct comparison of theory and modelling with experimental observations of ELM dynamics play an important role. The measurements performed with Electron Cyclotron Emission Imaging (ECEI) diagnostic on KSTAR [2,3,4] provided insights on the dynamics of ELM instability. In particular the rotating structures with medium toroidal mode numbers ( $n=5-8$ ) lasting about few milliseconds in time were detected in the pedestal region inside separatrix in the inter-ELM period and prior to the ELM crash (so called “precursor” phase). The observed modes rotate with the frequencies of order of the diamagnetic one (5-30kHz). Moreover a rapid change of the dominant mode number to another one or co-existence of few modes in the temperature fluctuation spectrum were detected on KSTAR using ECEI [4]. The direction of modes rotation on KSTAR can be both in electron and ion diamagnetic directions [2-4]. Similar observations were done on AUG [5], MAST [6], NSTX [7], however ELM precursors rotation was mainly in electron diamagnetic direction. Linear MHD modelling for KSTAR discharge parameters [3] suggested that the ballooning/peeling modes destabilized in the pedestal are good candidates to explain the ECEI diagnostic observations, however only linear stage was modelled and modes rotation was not explained in [3]. The observed regular

rotation of the modes decreases while approaching the ELM crash when ELM filaments cross the separatrix [2,7]. During ELM crash the expelled ELM filaments propagate in SOL and “blobs” are cut from the main plasma due to the strongly sheared poloidal mean flow generated on the highly non-linear phase of the ELM crash [8,9]. The rotating ELM precursors were modelled using non-linear MHD code JOEK in [9], where it was shown that before ELM crash the two fluid diamagnetic and electrostatic drifts produce poloidal rotation of the ballooning modes in the range of diamagnetic frequencies mainly in electron diamagnetic direction similar to most experimental observations [1, 5-7]. However only single harmonic was used and no direct comparison with experiment was done in [9]. In the present work we modelled ELM precursors and filaments dynamics for the realistic KSTAR pulse #7328 parameters [3] and compared to the ECEI observations. In particular it was demonstrated that only in multi-harmonics multi-cycle non-linear modelling including two fluid diamagnetic effects and toroidal rotation many experimental observations can be reproduced.

**2. Modelling results.** The detailed description of reduced resistive non-linear MHD code JOEK can be found in [8] and a model with two fluid diamagnetic and neoclassical effects we used here can be found in [9,10]. Here we just recall that the main flows used in present modelling. The normalized fluid velocity (for ions) in JOEK units [10] is taken in the

following form:  $\vec{V} = \underbrace{-R^2(\nabla u \times \nabla \varphi)}_{\vec{V}_{\vec{E} \times \vec{B}}} - \underbrace{\tau_{IC} \frac{R^2}{\rho}(\nabla p \times \nabla \varphi)}_{\vec{V}_i^*} + v_{\parallel} \vec{B}$ . Here the first term represents

the  $\vec{E} \times \vec{B}$  convection, the second term is the ion diamagnetic drift and the last one is the motion parallel to the magnetic field. Here  $u$  is the electrostatic potential,  $\rho$  - is the mass density normalized to the central value  $\rho_0$ ,  $p = \rho T = \rho(T_i + T_e)$  is the normalized scalar total pressure,  $T_{e,i}$  are the electron/ion temperatures,  $\varphi$  - is the toroidal angle and  $R$ -the major radius. The magnetic field is represented in the form:  $\vec{B} = F_0 \nabla \varphi + \nabla \psi \times \nabla \varphi$  [9,10], where  $\psi$  -is the poloidal magnetic flux, and  $F_0 = B_{\varphi,0} R_0$ ,  $B_{\varphi,0}$  being the toroidal field on the magnetic axis. For simplicity here  $T_e / T_i = 1$ , but the model is bi-fluid, since the electron diamagnetic terms are kept in Ohm's law [10]. The normalized parameter in diamagnetic term can be written as:  $\tau_{IC} = m_i / (2 \cdot e \cdot F_0 \sqrt{\mu_0 \rho_0})$ . For KSTAR parameters  $\tau_{IC} \sim 3 \cdot 10^{-3}$ . Both resistivity and viscosity are temperature dependent:  $\nu_{\parallel, \perp}, \eta \sim (T / T_{\max})^{-3/2}$ . The Lundquist number in the center was taken  $S = 8 \cdot 10^6$  which is for numerical reasons about two orders of magnitude smaller than the realistic value. The parallel conduction has a Spitzer-like temperature dependence:  $K_{\parallel} \sim K_{\parallel,0} (T / T_{\max})^{5/2}$ . The ratio to the perpendicular thermal conductivity for plasma center was taken  $K_{\parallel} / K_{\perp} \sim 10^8$ . The normalized coefficients for neoclassical poloidal viscosity were taken constant for simplicity as in [10]:  $\mu_{i,neo} = 2 \cdot 10^{-5}$ ;  $k_i = -1.1$ . A toroidal rotation source was introduced in the equation for parallel velocity to maintain the rotation profile at the initial value compensating losses due to the parallel viscosity ( $S_V = -v_{\parallel} \Delta V_{\parallel, t=0}$ ), normalized viscosities are  $\nu_{\parallel} = 10^{-5}$ ;  $\nu_{\perp} = 10^{-6}$ . The boundary conditions around the computational domain correspond to those of an ideally conducting wall where all perturbations vanish [8]. Bohm boundary conditions are set for the parallel velocity and parallel heat flux on the divertor target plates [8, 10].

Since the precise pedestal profiles measurements are not available on KSTAR here we used the same procedure as in [3]. The initial equilibrium for KSTAR pulse #7328,

$B_{tor}=2.25T$ ,  $I_p=750\text{ kA}$ ,  $q_{95}=5$  was calculated by EFIT code (EQDSK file) at time  $t=4.36s$ , but then pedestal pressure profile was modified similar to [3] and equilibrium was recalculated self-consistently using JOREK code. The initial density, temperature, pressure profiles used in modelling are presented in Fig.1. The toroidal rotation profile was taken close to the experimental one measured by CES diagnostic (Fig.2). For KSTAR pulse #7328 at time  $t=4.36s$  (corresponding to the inter ELM phase) the ECEI diagnostic detected structures localized on the Low Field Side (LFS) just inside separatrix with the main toroidal number  $n=8$  which were rotating poloidally with a velocity about  $V_{pol,exp}\sim 5.4\text{ km/s}$  (Fig.3). The first case of JOREK code modelling was done for a single harmonic  $n=8$  similar to [3], but including all relevant drifts and toroidal rotation. Both linear phase and highly non-linear phase of ELM crash leading to profiles relaxation were modelled.

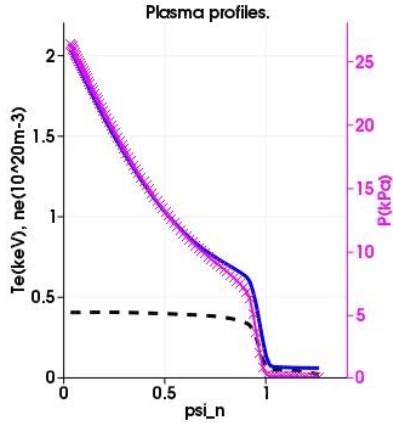


Fig.1 Initial density (dashed black), temperature (blue), pressure (cross magenta) profiles used in JOREK modelling.

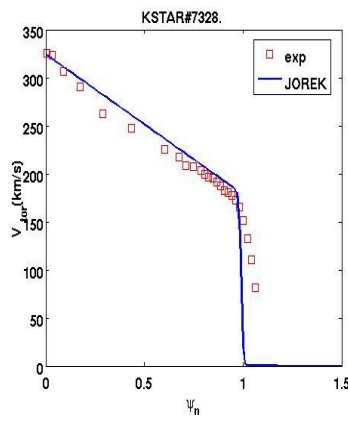


Fig.2 Toroidal rotation profile used in modelling (blue) and measured by CES diagnostic (red squares).

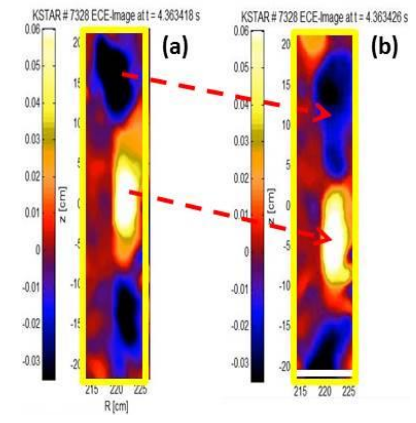


Fig.3. Two ECEI diagnostic images of temperature fluctuations before ELM crash separated by  $\sim 0.008\text{ ms}$  in time.

The time evolution of the magnetic energy of the single harmonic  $n=8$  calculated by JOREK is presented in Fig. 4. The  $n=8$  perturbations were initialized in the code at small amplitude ( $10^{-27}$ ). The temperature fluctuations for the  $n=8$  ballooning mode inside separatrix in the frame corresponding to the ECEI observation window are presented in Fig.5. Here (a) and (b) images taken just before ELM crash are separated by  $0.008\text{ ms}$  (two points in time indicated by diamonds in Fig.4). Note that mode rotates poloidally in the ion diamagnetic direction

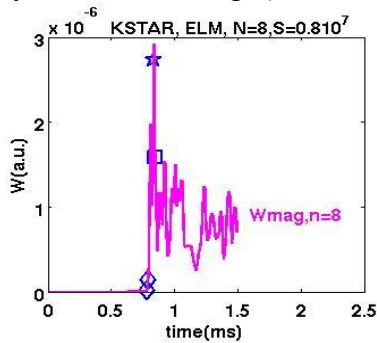


Fig.4 The time evolution of the magnetic energy of the single harmonic  $n=8$  during full ELM crash calculated by JOREK.

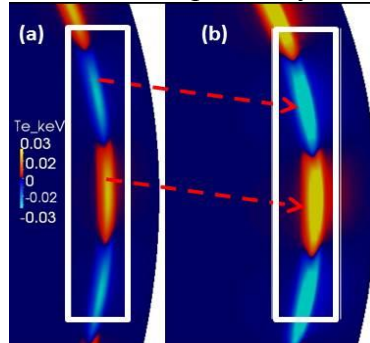


Fig.5. Two images of temperature fluctuations before ELM crash separated by  $\sim 0.008\text{ ms}$  in time in JOREK modelling in single harmonic  $n=8$  simulation at  $V_{tor}=325\text{ km/s}$

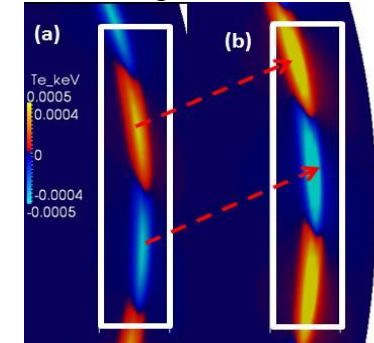


Fig.6. Two images of temperature fluctuations before ELM crash separated by  $\sim 0.008\text{ ms}$  in time in JOREK modelling in single harmonic  $n=8$  simulation at  $V_{tor}=54\text{ km/s}$

(here clockwise direction) at about  $\sim 5\text{ km/s}$  which is similar to the experimentally observed  $\sim 5.4\text{ km/s}$ . As it was demonstrated in [9] the poloidal rotation frequency of the ballooning

mode in the frame rotating with plasma follows typically ideal MHD predictions and is the order of a half of the ion diamagnetic frequency in the ion diamagnetic direction. However in the laboratory frame the rotation of the plasma itself should be taken into account. Mode  $(m,n)$  frequency in a laboratory frame should include Doppler shift due to plasma poloidal and toroidal rotation and can be expressed in a form:  $f_{\theta,mode} \approx mf_{\theta,pl} + nf_{\phi,pl} + 0.5mf_i^*$ , where  $f_{\theta,pl}, f_{\phi,pl}$  are poloidal and toroidal plasma rotation frequencies respectively and  $f_i^*$  is ion diamagnetic frequency, which for circular plasma is:  $f_i^* \approx V_{\theta,i}^* \cdot m / (2\pi r)$ , where  $r$  is minor radius of mode location. The poloidal velocity of the mode can be approximated for circular plasma as:  $V_{\theta,mode} \sim 2\pi r / m \cdot f_{\theta,mode}$ . Using also the approximation for a safety factor  $q_{res} = (m/n) \approx (RB_{\theta}) / (rB_{\phi}) = R / rb_{\theta}$  one can write the approximate expression for the poloidal velocity of the mode in the laboratory frame as:  $V_{mode(m,n),lab} \approx V_{\theta,pl} + V_{\phi} b_{\theta} + 0.5V_{\theta,i}^*$  where  $V_{\theta,pl} = V_{\theta,E \times B} + V_{\theta,i}^*$ . The observed poloidal rotation of the mode can be in electron or in ion diamagnetic direction depending on the pedestal plasma parameters [9]. In particular at relatively low toroidal rotation the mode generally rotates in the electron diamagnetic direction since the dominating term is  $V_{E \times B}$  due to the existence of the large negative radial electric field “well” in the pedestal region [9]. This situation is most typical on most of tokamaks. However at higher plasma toroidal rotation, the direction of modes rotation can change to the ion diamagnetic direction as it is the case in KSTAR pulse #7328 (Fig.3) analyzed in the present paper and reproduced in JOEUK modelling (Fig.3, 5). To check this conclusion we did a run with the same form of the toroidal velocity profile but reduced central value:  $54\text{km/s}$  instead of experimental  $325\text{km/s}$ . As a result before ELM crash mode  $n=8$  was rotating poloidally in electron diamagnetic direction at  $\sim +7\text{km/s}$  (Fig.6). The poloidal velocities profiles estimated using approximated formula presented above are shown in Fig.7. Note that the direction of the poloidal rotation of the mode  $n=8$  changes from ion diamagnetic direction at large experimental-like toroidal rotation ( $325\text{km/s}$ ), to electron diamagnetic direction at relatively low toroidal rotation ( $54\text{km/s}$ ).

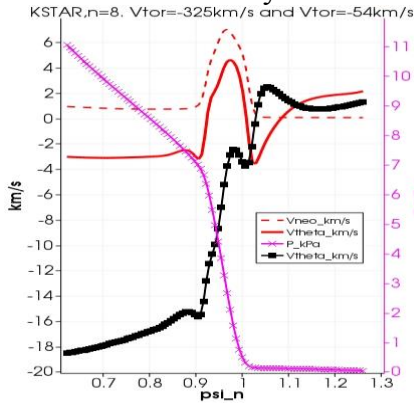


Fig.7 Poloidal velocities at mid-plane LFS for  $n=8$  mode on the linear phase (

$$V_{(m,n),lab} \approx V_{\theta,pl} + V_{\phi} b_{\theta} + 0.5V_{\theta,i}^* )$$

Pressure profile (magenta cross),

velocity of the mode at

$V_{tor} 54\text{km/s}$  (red, bold), at

$V_{tor} = 325\text{km/s}$  (black squares),

neoclassical poloidal velocity of ions is  $V_{neo}$  (dashed, red).

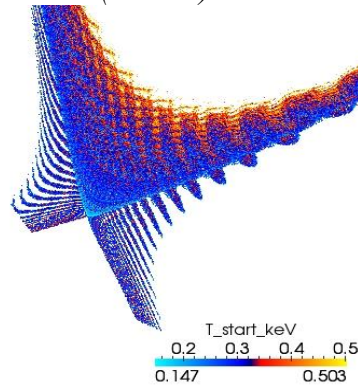


Fig.8. Magnetic topology produced by  $n=8$  ballooning mode destabilization at a time corresponding to a maximum of magnetic energy (indicated by star in Fig.4)

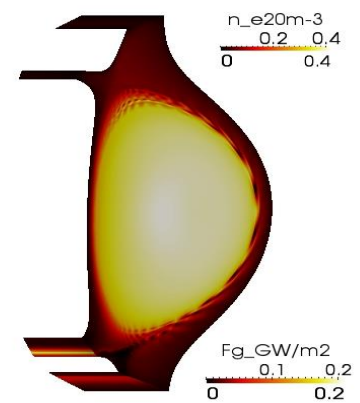


Fig.9 Density filaments during non-linear phase of an ELM and maximum heat flux in the inner and outer divertor due to an ELM.



At the non-linear phase of an ELM the magnetic perturbation is strong enough to force reconnections leading to the edge ergodic region formation [8]. The magnetic topology during ELM crash near X-point at the time corresponding to the maximum of the magnetic energy (indicated by a star on Fig.4) is presented in Fig.8. The density filaments expelled from the main plasma at this time are presented in Fig.9. Snapshots of the temperature perturbations before and just after ELM crash separated in time by  $\sim 0.0166ms$  are presented in Fig.10, where ECEI observation window is indicated by the vertical lines. Note the dramatic change in the mode rotation after the frame (4) in Fig.10. This time corresponds to the maximum of the magnetic energy for the mode  $n=8$  (indicated by a star in Fig.4) where actually the ELM crash starts. Approaching the crash the regular rotation of the mode first decreases (frames 1-4 in Fig.10) and then the rotation of the electron temperature perturbations becomes irregular and can change the direction and the amplitude in the narrow layers within the pedestal. The dynamics of ELM filaments at this stage is mainly defined by a strongly sheared mean poloidal flow which is generated due to the non-linear mode coupling via Maxwell stress tensor [8,9]. The poloidal plasma velocity profile during an ELM is presented in Fig.11. Note narrow layers of strong shear in the poloidal flow structure. As a consequence the expelled filaments are cut from the main plasma forming “blobs” (Fig.9-10). On the non-linear phase of an ELM the density and temperature profiles are relaxed (Fig.12).

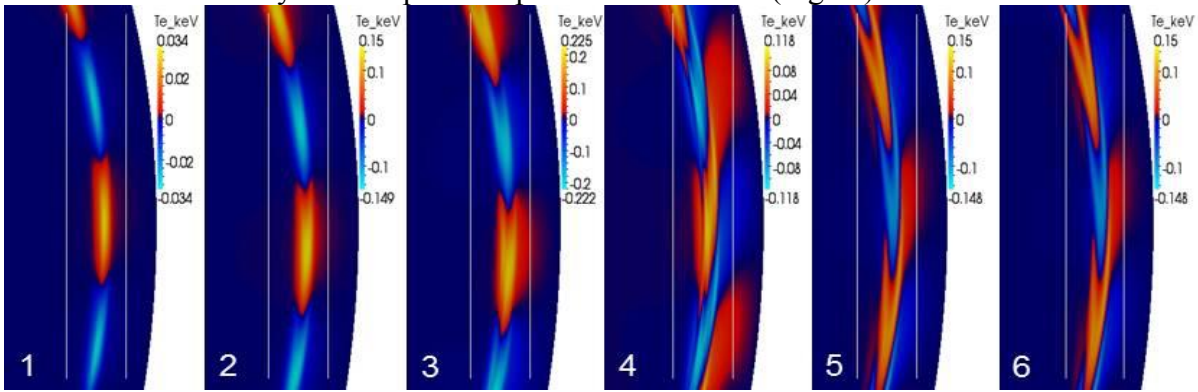


Fig.10. Snapshots of temperature fluctuations in the mid-plane on LFS before and during ELM crash. Images are separated in time by  $\sim 0.0166ms$

Note that in spite of the ballooning structure of the mode and its initial localization on the LFS, more ELM power is deposited into the inner divertor (Fig.9) which is typical feature observed in modelling including drifts [11] and in many experiments [12].

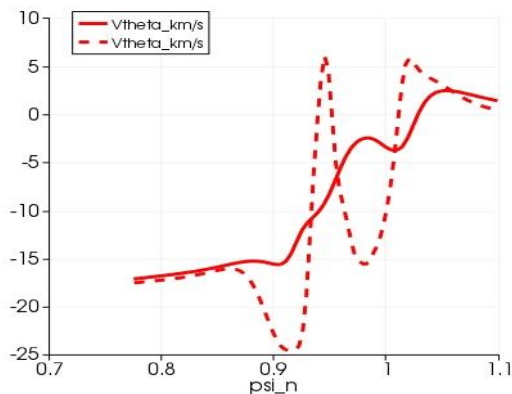


Fig.11 Poloidal velocity profile at mid-plane on LFS. . Before an ELM (time of the frame “1” in Fig.10 )-in bold, During non-linear phase (time corresponds to the frame “4” in Fig.11) -in dashed.

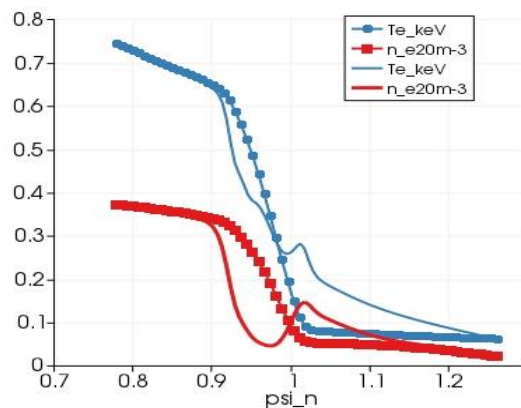


Fig.12. Relaxation of density (in red) and temperature (in blue) profiles during an ELM (modelling with single harmonic  $n=8$ ). Profiles before ELM crash (with markers) correspond to the frame “1” and after crash (plain lines) to the frame “6” in Fig.10.

The single harmonic modelling described above showed that if the ballooning mode is unstable, its structure, localization in the pedestal and poloidal rotation velocity are very similar to the ECEI observations in the pedestal region on KSTAR. However note that not all “precursors” observed in experiment lead to an ELM crash and typically several coherent modes lasting few  $ms$  are observed at the same time in temperature fluctuation spectrum in the inter-ELM periods [4], which can’t be explained in single harmonic and single ELM simulation presented above. To consider more realistic conditions multi-mode and multi-ELM cycles were studied in this work. In the Fig.13 magnetic energies of  $n=1-8$  modes are presented for the JOREK run for the same parameters (Fig.1-2), but in multi-harmonics regime. One can see that  $n=8$  mode remains the most unstable and other modes  $n=4-7$  are also linearly unstable, but with smaller growth rates than  $n=8$  (Fig.13). Approaching the non-linear phase all modes became strongly coupled. Note in particular that  $n=1-3$  modes (dashed lines in Fig.13) which were linearly stable in initial stage became unstable in the non-linear phase. This is similar to the findings of low- $n$  structures induced by non-linear coupling in multi-harmonic ELM modelling presented in [13]. The spectrum of temperature fluctuations in the inter-ELM period after a crash (Fig.14) showed a presence of the coherent modes  $n=5-8$  during few  $ms$ . Note that the dominant harmonic number can change in time during the pedestal build-up in modelling, which is similar to ECEI observations [4].

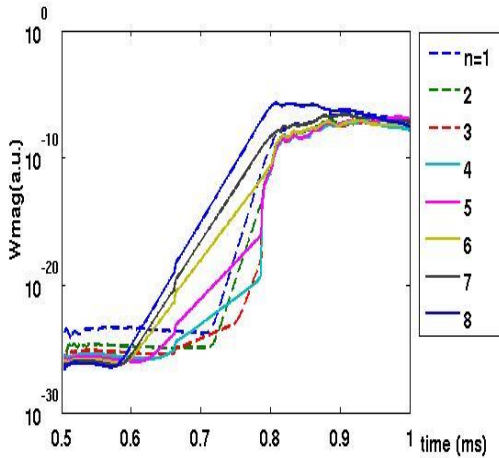


Fig.13. Magnetic energy in multi-harmonics ( $n=1-8$ ) simulation of ELM in KSTAR. Dashed lines indicate initially linearly stable, but then non-linearly unstable modes ( $n=1-3$ ).

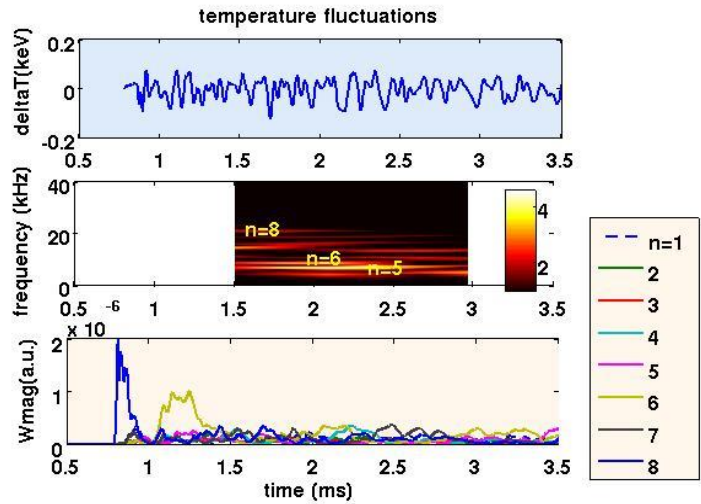


Fig.14. Temperature fluctuations in the pedestal at mid-plane in JOREK modelling (upper frame), frequency spectrum (middle), magnetic energy in time (bottom) for multi-harmonics simulation of an ELM on KSTAR for  $V_{tor}=325km/s$ .

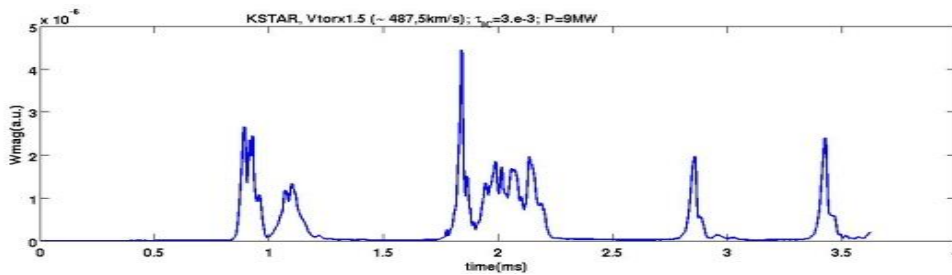


Fig.15. Magnetic energy versus time for multi-cycles simulations for single harmonic  $n=8$ ,  $V_{tor}=487km/s$ , NBI power was taken 9MW.

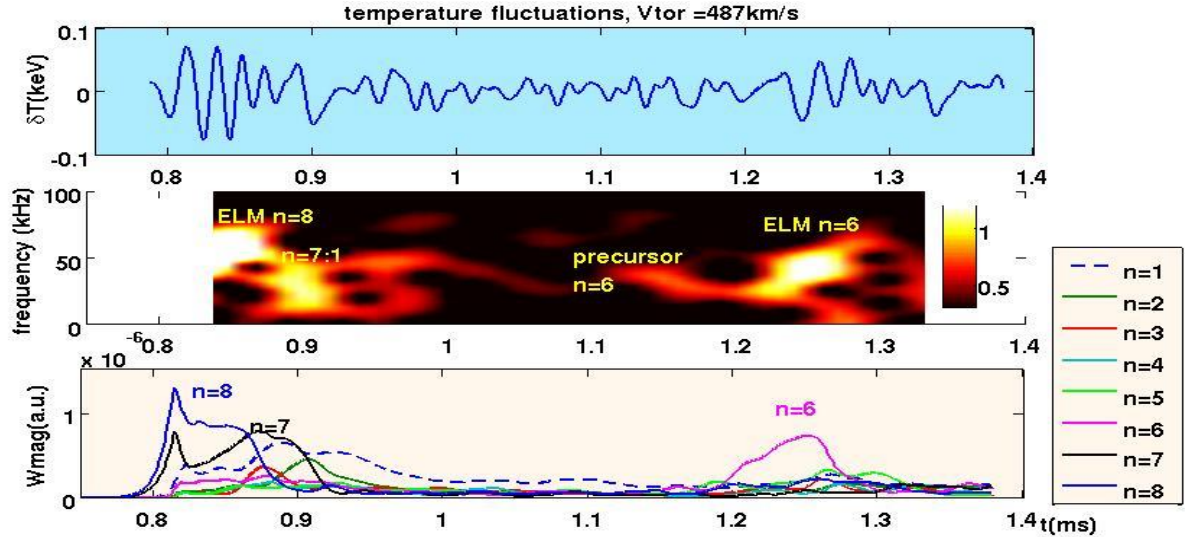


Fig.16. Temperature fluctuations in the pedestal at mid-plane in JOREK modelling (upper frame), frequency spectrum (middle) and evolution of the magnetic energy in time (bottom) for multi-harmonics simulation ( $n=1-8$ ) of an ELM at increased  $V_{tor}=487 \text{ km/s}$  and  $9 \text{ MW}$  NBI power.

The experimental ELM frequency for pulse KSTAR#7328 was about  $40 \text{ Hz}$ , hence inter-ELM period  $\sim 25 \text{ ms}$ . This is too long inter-ELM period for the modelling, since multi-harmonics are highly time and memory consuming and the time step in inter-ELM period should be kept of order of few Alfvén times ( $\sim 10^{-4} \text{ ms}$ ) to resolve all harmonics fluctuations in time. In order to achieve multi-harmonics and multi-ELM regime on more reasonable and shorter time accessible for modelling the heating power was artificially increased:  $9 \text{ MW}$  in modelling instead of  $3 \text{ MW}$  in experiment. At the same time toroidal velocity was increased ( $487 \text{ km/s}$  instead of  $325 \text{ km/s}$  in experiment) to increase the stabilizing effect of the rotation on the remaining MHD after ELM crash which permits the pedestal re-built on a shorter time scale similar to [11]. This case is presented in Fig.15, where  $1.2 \text{ kHz}$  ELMs were obtained using  $n=8$  single harmonic and  $1.7 \text{ kHz}$  ELMs for multi-harmonics  $n=1-8$  case (Fig.16 bottom frame). Note that in case of multi-harmonics the second ELM is due to  $n=6$  mode compared to the first  $n=8$  ELM. The frequency spectrum of the electron temperature fluctuations for this case is presented in Fig.16 (middle frame), showing  $n=6$  precursor prior to the second ELM lasting about  $\sim 0.15 \text{ ms}$ .

**3. Discussion and conclusions.** The non-linear MHD modelling of full ELM crash dynamics was done using JOREK code with two fluid diamagnetic and neoclassical effects [8,10] for KSTAR pulse #7328 parameters and compared to the ECEI diagnostic observations [3]. Most of the experimentally observed features were reproduced in modelling. In particular the structure and localization of the medium  $n$  ( $n=5-8$ ) peeling-ballooning modes in the pedestal region inside the separatrix, poloidal rotation frequencies and the direction of the modes rotation before ELM crash are similar to the experimental observations using ECEI on KSTAR. It was shown that observed poloidal rotation can be in electron diamagnetic direction (more common observation in many tokamaks [5-7]) and in ion diamagnetic direction at relatively large toroidal rotation which was the case for the KSTAR [3-4] pulse modeled in the paper. On the highly non-linear phase of ELM crash the regular rotation of the modes decreases and ELM filaments are expelled to the SOL. More ELM power is found in the inner divertor (in/out = 2:1) compared to the outer divertor with two fluid diamagnetic and  $\vec{E} \times \vec{B}$  drifts included in the model [11] which is similar to the experimental findings [12]. Multi-modes ( $n=1-8$ ) modelling demonstrated acceleration of growth of all peeling-ballooning modes and the destabilization of the previously linearly stable modes while

approaching the ELM crash. This is due to the strong non-linear coupling of the modes in this phase as it was also found in [13]. In multi-ELMs regimes in the inter-ELM periods and before ELM crash the temperature fluctuations spectrum in modelling is similar to one observed in experiment. In particular the presence of several unstable modes ( $n=5-8$ ) in the range of frequencies ( $5-20kHz$ ) were obtained. The time duration of these coherent structures varies from  $0.15ms$  to  $2ms$  in modelling. Note however that this work did only a first step in the interpretation of the experimental observations of ELM precursors and obviously has its limits. In the first place the exact pedestal measurements were not available on KSTAR, so there was a certain freedom in a choice of the pedestal pressure and its gradient which defines a diamagnetic velocity value. The resistivity in modelling for numerical reasons was two orders higher in modelling than in experiment. At the realistic resistivity the linear growth rate of the modes probably will change. Limitations in the computer time and memory for multi-harmonics simulations did not permit to achieve realistic experimental ELM frequency. Note however that the aim of this work was mainly to propose a minimum model for the possible underlying mechanism of the observed rotating structures in the pedestal temperature before ELM crash (ELM precursors) and in the inter-ELM periods.

### References:

- |   |   |
|---|---|
| [1] A Loarte et al Plasma Phys. Contr. Fusion <b>45</b> , 1549 (2003) | [8] G T A Huysmans et al Nucl. Fusion <b>47</b> ,659 (2007)             |
| [2] G Yun et al Phys Rev Lett <b>107</b> ,045004(2011)                | [9] J Morales Phys of Plasmas <b>23</b> ,042513(2016)                   |
| [3] M. Kim et al Nucl. Fusion <b>54</b> , 093004 (2014)               | [10] F Orain et al Phys of Plasmas <b>20</b> , 102510 (2013)            |
| [4] J E Lee et al Nucl Fusion <b>55</b> , 113035(2015)                | [11] F Orain et al Plasma Phys Control Fusion, <b>57</b> , 014020(2015) |
| [5] I Classen et al Nucl Fusion <b>52</b> ,1223009 (2012)             | [12] R A Pitts et al Nucl. Fusion <b>47</b> (2007) 1437–1448            |
| [6] A Kirk et al Nucl Fusion <b>54</b> ,114012(2013)                  | [13] I Krebs et al Physics of Plasmas, <b>20</b> , 082506 (2013)        |
| [7] Y Sechrest et al Nucl Fusion <b>52</b> ,123009(2012)              |   |

**Acknowledgement:** *This work has been carried out within the framework of the EUROfusion Consortium and has received funding from grant AWP15-ENR-01/IPP-05. A part of this work was carried out using the HELIOS supercomputer system (IFERC-CSC), Aomori, Japan, under the Broader Approach collaboration, implemented by Fusion for Energy and JAEA. The part of this work was carried out using MARENOSTRUM supercomputer system (Barcelona, Spain) under PRACE project (2016) and also partly using HPC CCRT-CURIE partly using HPC CURIE (TGCC-Bruyères-le-Châtel, France) under GENCI project(2016). The views and opinions expressed herein do not necessarily reflect those of the European Commission or ITER.*